Experimental exergy analysis of R513A to replace R134a in a small capacity refrigeration system

Adrián Mota-Babiloni[a], J.M. Belman-Flores[b*], Pavel Makhnatch[c],

Joaquín Navarro-Esbrí[a], J.M. Barroso-Maldonado[b]

[a] *ISTENER Research Group, Department of Mechanical Engineering and Construction, Universitat Jaume I, Av. de Vicent Sos Baynat, 12071 Castellón de la Plana, Spain*

[b] *School of Engineering Campus Irapuato-Salamanca, University of Guanajuato, Carretera Salamanca-Valle de Santiago km 3.5+1.8 Comunidad de Palo Blanco, Salamanca, 36885 Guanajuato, Mexico*

[c] *Division of Applied Thermodynamics and Refrigeration, Department of Energy Technology, The Royal Institute of Technology (KTH), Brinellvägen 68, SE-10044 Stockholm, Sweden*

* Corresponding author.

Tel.: +52 (464) 6479940 Ext. 2419; fax: +52 (464) 6479940 Ext. 2311

E-mail address: jfbelman@ugto.mx (J.M. Belman-Flores)

Abstract

The replacement of HFCs using lower GWP refrigerants in the coming years is a priority to reduce the predicted climate change. The exergy analysis of vapor compression systems can help to identify the feasibility of alternative fluids in existing installations and the potential to improve them. In this sense, this paper presents an exergy analysis of an experimental setup which operates with R134a and the alternative HFO/HFC mixture R513A. The evaporating temperature is ranges between -15°C and 5°C, while the condensing temperature is set at 30°C and 35°C. In this analysis, the highest amount of exergy destruction rate is obtained at the compressor, followed by the evaporator. The maximum exergy efficiencies are observed at the condenser and the thermostatic expansion device. Finally, the average global exergy efficiency of R513A when replaced R134a in this refrigeration experimental setup is 0.4% higher (absolute difference), and with respect to the components, there is only slight reduction in efficiency in the condenser using R513A. Therefore, the R513A replacement is acceptable according to the second law of thermodynamics.

Keywords: vapor compression; second law of thermodynamics; exergy destruction rate; global warming potential; R513A.

Nomenclature

$\dot{E}_d$	Exergy destruction rate [W]
e	Specific exergy [J kg^{-1}]
h	Specific enthalpy [J kg^{-1}]
$\dot{m}$	Mass flow rate [kg s^{-1}]
$\dot{Q}$	Heat losses [W]
s	Specific entropy [J kg^{-1} K^{-1}]
T	Temperature [K, °C]
$\dot{W}$	Electric power [W]

Greek symbol

η_{ex}	Exergy efficiency

Subscripts

brine	Secondary fluid (evaporator)
comp	Compressor

c, cond	Condenser
dis	Discharge line
evap	Evaporator
in	Inlet
out	Outlet
ref	Refrigerant
suc	Suction line
water	Secondary fluid (condenser)
0	Equilibrium state

Abbreviations

Ave	Average
COP	Coefficient of performance
GWP	Global Warming Potential
HFC	Hydrofluorocarbon
HFO	Hydrofluoroolefin
IHX	Internal Heat Exchanger
Max	Maximum
Min	Minimum
TXV	Thermostatic Expansion Valve
wt%	Weight percentage

1. Introduction

Hydrofluorocarbons (HFCs) phase-down is a priority in the reduction of the predicted increase of the Earth's surface mean temperature. The Kigali Amendment to the Montreal Protocol [1] and the Regulation (EU) No 517/2014 [2] are the two more relevant legislation enforcing this process, until today. The Kigali Amendment establishes a calendar to perform a drastic reduction of the HFCs worldwide. The EU Regulation started in 2015 to phase down HFCs while also gradually banning those with high Global Warming Potential (GWP) from the most extended domestic and commercial refrigeration and air conditioning applications. R134a, with a GWP of 1300, is one of the most extended refrigerants today and it is going to be retired in Europe from such applications as domestic refrigerators and freezers, supermarket multipack systems and mobile air conditioners [3]. Moreover, due to the restrictions in

HFCs consumption quota or, in some countries, fluorine fluids taxes, R134a price is increasing.

A significant amount of investigations about HCFCs and HFCs (especially R134a) substitution, using natural refrigerants (particularly carbon dioxide and hydrocarbons) and other synthetic refrigerants are being carried out to propose solutions in the face of the negative consequences of the global warming [4,5]. The first developed synthetic low GWP refrigerants to replace R134a were R1234yf [6] and R1234ze(E) [7]. Both fluids are hydrofluoroolefines (HFOs), they have low GWP values below 1 [8] and they are low flammable fluids [9–11]. After several theoretical and experimental studies, the operational advantages and disadvantages of these fluids were proved: R1234yf does not improve the energetic performance of refrigeration and air conditioning applications [6,7] and R1234ze(E) requires large modifications or new design systems to reach the cooling capacity of the refrigeration system [12].

A few mixtures of both types of fluids, HFCs and HFOs, have been developed and commercialized to mitigate the drawbacks of the pure HFOs and obtain a working fluid with a lower GWP value than R134a. R450A and R513A are obtained by mixing R134a with R1234ze(E) and R1234yf, respectively. They have a lower GWP values (547 and 562 for R450A and R513A, respectively), are low toxicity and non-flammable refrigerants, so they have been developed to cover air conditioning and refrigeration applications with safety. However, the energy performance of the refrigeration system and components has been studied with less coverage than that of the pure HFOs, due to the recent development of both refrigerants, and hence a few studies are available today [13–17].

R450A and R513A studies conclude that these alternative fluids present comparable refrigeration coefficient of performance (COP) than R134a at typical operating conditions when performing a drop-in or light retrofit replacement [3]. Available papers focus on the energy analysis (first law of thermodynamics) of HFC/HFO mixtures but do not include the effects of the replacement that can present the exergy analysis (second law of thermodynamics). The exergy analysis helps to better and accurately identify the location of inefficiencies [18] and, for instance, can also be used to improve the control of vapor compression systems and to establish the optimum operating conditions [19]. Most of the papers that compare the exergy efficiency and destruction rate in vapor compression system and components of R134a with alternatives consider hydrocarbons [18] or, more recently, the pure HFO fluids R1234yf and R1234ze(E).

For vapor compressor systems, according to the simplified model of Özgür et al. [20], R1234yf can be assumed as a more favorable refrigerant from the point of view of thermodynamics. Golzari et al. [21] modeled R1234yf and R134a global exergy efficiency and COP in a mobile air conditioning system showing higher global exergy efficiency for R1234yf. However, in a two-evaporator refrigeration system, Yataganbaba et al. [22] concluded that the R1234yf global exergy efficiency is slightly below than that of R134a. In the experimental mobile air conditioning system, Cho and Park [23] obtained between 3.4 and 4.6% lower R1234yf second law efficiency than the R134a system at all compressor speeds (800–1200 rpm). They also found that the internal heat exchanger (IHX) significantly improves the global exergy efficiency of the R1234yf refrigeration system between 1.5 and 4.6%. Belman-Flores et al. [24] tested R1234yf in R134a domestic refrigerators, the poorer global exergy efficiency for the R1234yf does not suggest this fluid as a drop-in replacement for R134a. System redesigns or refrigerant charge optimization is needed to replace the HFC.

Global exergy efficiency results with the other R1234ze(E) are more positive. In the walk-in room measurements performed by Kabeel et al. [25], the second law efficiency of the cycle operated with R1234ze(E) is nearly 17% higher than that of R134a. The two-evaporator model by Yataganbaba et al. [22] shown comparable performance between R1234ze(E) and R134a, but it requires a slight modification in the design to replace the HFC. In chillers, Ben Jemaa et al. [26] also concluded that the energy and the exergy efficiencies of both refrigerant cycles have almost the same values or even higher for R1234ze(E). In the theoretical study of Pérez-García et al. [27], R1234ze(E) was found to be the most efficient alternative to R134a, even with the integration of the IHX.

Additional information to the energy analysis of lower HFO/HFC GWP mixtures, therefore exergy analysis of the operation of the refrigeration system is needed to obtain a deeper analysis of the effects of substitution of R134a using these alternatives. This paper studies and discusses the global exergy efficiency and exergy destruction rate when R513A is used in a R134a installation at a wide range of operating conditions. R513A has been selected due to the promising results in the previous first law efficiency results [14]. The data used for this work is obtained from steady-state tests performed in a small capacity refrigeration experimental setup, varying the evaporation temperature from -15°C to 5°C and at condensation temperatures of 30°C and 35°C. The results of exergy efficiency and exergy destruction rates are discussed for the global installation, and its particular components.

2. Characteristics of R513A and R134a

Table 1 shows the main properties of the refrigerants under study in this work. It can be seen that the properties are very similar between refrigerants, especially regarding the ASHRAE safety classification, critical temperature and pressure, normal boiling point and liquid density. Furthermore, the R513A is considered an azeotropic refrigerant due to the negligible temperature glide and stands out the lower R513A GWP value in comparison with that of R134a. Additional information regarding other R134a refrigerants can be found in [3].

Table 1. Main characteristics of 513A and R134a.

3. Methodology

3.1. Experimental setup

A small capacity refrigeration test bench is used to have an accurate representation of the exergy performance of the vapor compression system using lower GWP mixtures alternatives to R134a, being selected in this case R513A. The test bench and scheme that present the main components of this system are shown in Figure 1.

Figure 1. a) Experimental setup and b) schematic diagram of its main components.

The compressor is a hermetic rotary type, with a nominal power of 550 W and a swept volume of 15.4 cm^3. Then, plate heat exchangers (channel volume of 0.062 dm^3) are used for condenser and evaporator, with an exchange area of 0.248 m^2 and 0.558 m^2, and 10 and 20 number of plates, respectively. The thermostatic expansion valve (TXV) controls the flow through the circuit, and it is designed for R134a. Heat exchangers, secondary elements, and circuit pipes are isolated to have a better reliability of the measurements. The condenser and the evaporator secondary circuits use water (open loop) and 43 wt% ethylene glycol-based solution (closed loop), respectively. A water regulating valve is adjusted to fix the condensing pressure at the target value, and three phase power resistances immersed in an isolated tank establishes the amount of heat transferred in the evaporator (2 x 810 W fixed, and 1 x 970 W adjustable, nominal values).

Temperature, pressure, mass flow rate, power and heaters power use are measured according to the information shown in Table 2. A data acquisition system collects these

measurements and transfers to a personal computer, in which the data are displayed and stored every 10 seconds. The rest of the steady-state output parameters are obtained using properties given by the REFPROP v9.1 database [28].

Table 2. Measurements collected in the experimental refrigeration setup.

3.2. Tests procedure

The steady-state test is recorded over a period of around 30 min. The pressures must be within an interval of ±2.5 kPa and the temperatures within ±0.5 K to consider the steady-state condition in a test. Then, once a steady state is recorded, the data used to represent the operating condition targeted are obtained averaging the most stable period of 10 min (being considered 60 direct measurements for each parameter mentioned in Table 2). The performed tests are intended to simulate a small capacity refrigeration system operating conditions at typical medium evaporating temperature, between -15°C and 5°C. The selected condensing temperatures are 30°C and 35°C and the maximum deviation allowed was ±0.2 K.

3.3. Exergy analysis

The exergy of a system is defined as the maximum theoretical work obtained during a process in which the system reaches an equilibrium state at environmental conditions. The exergy method analysis is based on the second law of thermodynamics and allows the designers to identify a location, cause, and magnitude of losses in thermal systems. Therefore, the exergy analysis can be used to evaluate the performance of a refrigeration system by determining the magnitude and location of the process' irreversibility.

By applying the first and second laws of thermodynamics, the general expression of exergy balance in any control volume is shown in Eq. (1) [29].

$$\dot{E}_d = \sum \left(1 - \frac{T_0}{T}\right) \dot{Q} - \dot{W}_{in} + \sum_{in} \dot{m}e - \sum_{out} \dot{m}e \qquad (1)$$

In this exergy balance, the exergy destruction rate, $\dot{E}_d$, represents a real loss in the quality of energy that cannot be identified by means of energy balance. In this study, the overall exergy destruction rate for the small refrigeration system is calculated considering the accumulation of the exergy destruction rate in each component, Eq. (2).

$$\dot{E}_{d,system} = \dot{E}_{d,comp} + \dot{E}_{d,cond} + \dot{E}_{d,TXV} + \dot{E}_{d,evap} \quad (2)$$

For the specific exergy referred to the working fluid of the refrigeration system, the kinetic and potential energy effects are neglected. Then, the specific exergy is defined in Eq. (3). In this equation enthalpy, h_0, and entropy, s_0, are measured in respect to a dead state conditions, 101.3 kPa and 298.15 K.

$$e = (h - h_0) - T_0(s - s_0) \quad (3)$$

The global exergy efficiency quantifies the relative losses in the overall refrigeration system and can be calculated as the ratio between the minimum power required by a reversible system and the exergy expenditure, Eq. (4).

$$\eta_{ex} = 1 - \frac{\dot{E}_{d,component}}{exergy\ expenditure} \quad (4)$$

For the overall vapor compression system, the exergy expenditure is represented by the actual power supplied to the compressor, Eq. (5).

$$\eta_{ex} = 1 - \frac{\dot{E}_{d,system}}{\dot{W}_{comp}} \quad (5)$$

In accordance with the above, the equations used to determine the exergy efficiency and the exergy destruction rate in the main components of the small capacity refrigeration system are shown in Table 3. The calculation of these parameters in each component allows identifying the possibilities of thermodynamic improvement of the system.

Table 3. Exergy destruction rate and efficiency equations for each component analyzed.

The exergy balance applied to the compressor involves the exergy transferred to the surroundings by heat transfer. In this case, the wall temperature, T_{wall}, is the boundary temperature located on the wall of the compression shell of the compressor. This temperature was defined by experimental data resulting in an average value of 77 °C. For the exergy efficiency of heat exchangers (see Eq. 4), the exergy expenditure is defined as the difference between the exergy of the refrigerant entering and leaving the heat exchanger. The heat transfer to the surroundings for the expansion valve was neglected because the dimensions of this component are relatively small.

4. Results and discussion

With the physical foundations mentioned above, the experimental data were used to simulate the exergy performance. The mathematical expressions were programmed in MatLab software, which was linked with REFPROP [27] for the estimation of thermophysical properties. Therefore, in this section the main results of the exergy analysis to a small refrigeration system are shown when the evaporation temperature varies from -15°C to 5°C (according to operating conditions) for both R134a and R513A refrigerants, setting two condensing temperature conditions (30°C and 35°C).

The global exergy parameters are displayed, then, the exergy efficiency and the exergy destruction rate results for the four main components of the refrigeration system (compressor, condenser, expansion device, and evaporator) are discussed. In order to expand the comprehensive analysis of the information presented in Figures 2, 4, 5, 6 and 7, the calculated uncertainty [30] of exergy efficiency and exergy destruction rate for the global refrigeration system and its four main components is reported in Appendix A.

4.1. Global exergy parameters

Figure 2 shows the behavior of the global exergy efficiency and the exergy destruction rate of the refrigeration system. Thus, Figure 2a depicts that the global exergy efficiency, after reaching a peak (between -15°C and -7°C), decreases slightly with the increase of the evaporation temperature (above -7°C). On the contrary, the global exergy destruction rate increases when the evaporating temperature rises (see Figure 2b). Figure 2 also shows the influence of the condensing temperature, which has a great effect on the exergy performance of the refrigeration system. With the increase in condensing temperature, the values of global exergy efficiency decreased. Therefore, the exergy destruction rate increases with the increase in condensing temperature for both refrigerants, because of the higher temperature difference between the ambient and the component.

The exergy balance of second law for the whole cycle would indicate that the exergy contribution towards the system is supplied by the power to the compressor and the cooling capacity in evaporator, and this accumulation is distributed in three terms: exergy loss to the water in condenser, exergy loss to the ambient because of heat dissipation throughout the compressor shell, and the exergy destruction rate. The evaporating temperature affects slightly the power consumption and significantly the cooling capacity. Then, given that the condensing temperature is kept constant (30°C

and 35°C), the heat transfer to the water does not change significantly. The result of this conceptual analysis confirms that R513A shows behaviors close to R134a: the greater the evaporating temperature, the greater the cooling capacity supplied to the system and the greater the exergy destruction rate is experienced. Note that the cooling capacity is calculated multiplying the measured mass flow rate by the refrigerant enthalpy difference at the evaporator (also known as refrigerating effect) and the required heat is provided as described in Section 3.1.

Figure 2. Global exergy performance vs evaporation temperature.

According to Figure 2a, the peak exergy efficiencies are about 0.265 and 0.236 for R134a, and 0.264 and 0.245 for R513A (condensing temperatures of 30°C and 35°C, respectively). Those values are reached for R134a at -10°C and -5°C, and for R513A, at -10°C and 7.5°C (evaporation temperature). Therefore, in this test bench designed for R134a, R513A can obtain similar or better global exergy efficiency and confirms promising energy performance results presented in the previous first law analysis study [14].

The details of the exergy results for global and components are summarized in Tables 4 and 5, which showed minimum, maximum and average values for the two conditions of condensing temperature. Reviewing the tables, very similar behaviors can be confirmed between both refrigerants.

Table 4. Global and components exergy efficiency at 30°C condensing temperature.

Table 5. Global and components exergy efficiency at 35°C condensing temperature.

To illustrate the relevance of the exergy destruction rate in each component, Figure 3 shows the exergy flow diagrams of the refrigeration system working with R134a and R513A at the two different condensing temperatures selected and an evaporation temperature of 0°C. By inspection of this figure, it is evident that the irreversibilities of the components are very similar in both refrigerants. In addition, it can be graphically seen the relevance of the compressor losses in comparison with the other components, about half of the losses is generated in this component. Figure 3a shows that the condenser is the component that contributes to the least losses, this in comparison with the shown in Figure 3b, where the expansion valve is the component with the lowest

irreversibilities. This is due to the condensing temperature (30°C) is very close to ambient temperature, involving minor losses in the condenser.

Figure 3. Exergy flow diagram for the refrigeration system, at a) T_{cond}=30°C, b) T_{cond}=35°C.

The global exergetic efficiency results can be complemented with those previously published for the energy performance (first law of thermodynamics) in Mota-Babiloni et al. [14]. In this work, R513A showed slightly higher COP than R134a and the higher compressor electric power consumption was compensated by the cooling capacity. From a global energetic, exergetic and environmental point of view, R513A can be an appropriate substitute for R134a.

4.2. Components exergy parameters

To broaden the information on the exergy performance of the refrigeration system, in this subsection the behaviors for the main components are presented and discussed.

4.2.1 Compressor

Figure 4 depicts the exergy performance of the compressor as a function of evaporation temperature (-15°C to 5°C), and under two constant values of condensing temperature (30°C and 35°C). Figure 4a shows the increase in compressor exergy efficiency as the evaporation temperature rises. The exergy efficiency behavior of the compressor when working with refrigerant R513A is slightly higher with respect to R134a for different operating conditions of the refrigeration system. Although the compressor is designed for R134a, its exergy efficiency is noticeably higher for R513A. For instance, according to the results of Tables 4 and 5, for an average exergy efficiency the R513A represents 3.4% and 6.7% more than the R134a at condensing temperature of 30°C and 35°C, respectively.

This enlargement is produced despite the higher electricity power consumption presented in the previous paper [14]. The thermodynamic properties of this new mixture favor lower entropy production during the compression. The compressor exergy efficiency should be benefited at lower compression ratios. Also, the exergy efficiency in hermetic rotary compressors with a small capacity is low due to the existence of movable parts of the compressor and therefore this component is the most critical of all the analyzed, as observed in several papers found in the literature [21,22].

Additionally, Figure 4b shows the exergy destruction rate caused by the compressor. The increase of evaporation temperature decreases the exergy destruction rate. The compressor has a greater effect on the global exergy efficiency and exergy destruction rate. A higher compression ratio penalizes compressor efficiencies and hence global exergy efficiency. In addition, when the compression ratio increases, the temperature inside the compression chamber increase and hence more energy is dissipated due to the viscosity increase.

Figure 4. Exergy performance of the compressor, a) efficiency and b) destruction

4.2.2 Condenser

Figure 5 illustrates the influence of the evaporation and condensing temperatures on the exergy efficiency as well as on the exergy destruction rate of the condenser. The temperature range for secondary fluid (tap water) is between 17°C to 22°C for both refrigerants. As can be seen in Figure 5a, this component represents high exergy efficiency, and even more so at a low condensing temperature (30°C). In fact, the variation of the evaporation temperature does not greatly affect the exergy behavior of the condenser at low condensing temperatures. The exergy efficiency of the condenser is high because of two main reasons: first, the component is considered in adiabatic conditions (well insulated); and second, the condensing temperatures are very close to the ambient temperature (equilibrium conditions).

The new mixture is favored because of lower difference between the secondary fluid and refrigerant temperatures in the condenser. The R513A lower secondary condenser temperatures enlarge the heat transfer rate (and enlarge its condenser exergy efficiency) and reduce the exergy destruction rate (see Figure 5b). The condenser exergy efficiency increases with the reduction of the compression ratio and hence the condenser exergy destruction rate decreases. In this component, the exergy destruction rate diminishes and practically remains constant due to the decrease in the condensing temperature, which is close to those of reference state conditions.

Figure 5. Exergy performance of the condenser, a) efficiency and b) destruction.

4.2.3 Expansion valve

Figure 6 shows the TXV exergy efficiency and exergy destruction rate. As usually seen in the literature review, the TXV exergy efficiency values are the highest of the all the components of a refrigeration circuit and the throttling does not cause significant exergy destruction rate. The increase of evaporation temperature reduces the entropy production and hence the exergy destruction rate; this is reflected in the increment of the exergy efficiency for this component. No significant differences can be observed between both refrigerants and hence the R134a thermostatic expansion valve also has an appropriate design for R513A.

The valve's exergy destruction rate is small since the only effect considered is the variation in entropy between the two operating pressures, see Figure 6b. The exergy destruction rate is higher for R513A because of the high mass flow rate and the expansion valve entropy difference. Moreover, the pressure drop across the TXV is higher R513A than R134a for the same operating temperatures. As with the other components, the exergy destruction rate increases for higher condensing temperatures.

Figure 6. Exergy performance of the expansion valve, a) efficiency and b) destruction.

4.2.4 Evaporator

The exergy behavior of the evaporator is shown in Figure 7. The behavior of exergy efficiency and exergy destruction rate are very similar for both refrigerants under the operating conditions shown, Figure 7a. At higher evaporation temperatures, the evaporator exergy efficiency is similar to that of compressor and hence this evaporator is not properly designed to operate at those conditions, being more ideal this evaporator sizing for lower operating temperatures (lower difference between the secondary fluid and refrigerant temperatures in the evaporator, and mass flow rate), apart from the condensing conditions.

In the same way, Figure 7b shows as the evaporator exergy destruction rate grows considerably at higher evaporating temperatures because of the increase in the mass flow rate (which is associated with the increase in the cooling capacity and hence with the exergy transfer between the brine and refrigerant). Besides, the difference between both condensing temperatures considered is smaller, since only the volumetric

493 efficiency and the quality at the inlet of the evaporator are slightly varied. Hence, as the
494 pressure difference across the compressor and the expansion valve increases, this
495 component destroys more exergy. The maximum evaporator exergy destruction rate is
496 approximately half the measured at the condenser. Despite the higher pressure and
497 temperature of the refrigerant in the condenser, the temperature difference with the
498 secondary fluid is greater in the case of the evaporator and there is more difference
499 between its mean temperature and the ambient.
500
501 For the evaporator there is no significant influence of the condensation temperature on
502 the exergy destruction rate. Likewise, it is worth mentioning that the exergy destruction
503 rate does not present significant differences for both refrigerants in both the trends and
504 numerically, even though the evaporator was designed to operate only using R134a.

505
506 Figure 7. Exergy performance of the evaporator, a) efficiency and b) destruction.
507
508

509 **5. Conclusions**
510
511 In this paper, the experimental results on the exergy behavior of R513A versus R134a
512 were presented and discussed, considering the exergy efficiency and destruction in the
513 global system and the four main components. The analysis was developed using a data
514 set obtained from a small vapor compression system equipped with a full hermetic
515 rotary compressor. The comparison was carried out for evaporation temperatures ranged
516 between -15°C and 5°C and condensing temperature selected at 30°C and 35°C. Based
517 on this analysis, the following can be concluded:
518

519 - The global exergy efficiency of R513A was slightly higher than that of R134a,
520 despite R513A presented higher exergy destruction rate. The global efficiency
521 reached a maximum for a determined evaporating temperature and then was
522 reduced. This parameter was benefited from lower condensing (cooling water)
523 temperatures, especially for the new mixture R513A.
524 - The component that caused higher irreversibility and hence lower exergy
525 efficiency in this experimental system was the compressor, given the presence of
526 rotary parts and losses to the ambient. Condenser and expansion valve were the
527 components with the highest exergy efficiency, and the evaporator presented
528 intermediate values. Exergy destruction rate of the water-cooled condenser was

reduced, given the compact design of the plate heat exchanger that results in enhanced heat transfer rates, and the insulation.

- The second-law analysis confirmed that R513A does not need a redesign to be used in R134a refrigeration systems since the exergy efficiency in all the components was comparable to that of R134a or even higher. However, the rotary compressor should be replaced by another technology able to efficiently work with small cooling capacities to increase the final performance of the refrigeration system.

Acknowledgements

This research is done within the Effsys Expand P08 project that is funded by the Swedish Energy Agency with the support of Bosch Thermoteknik AB, Danfoss Värmepumpar AB, Nibe AB, Nowab, Svensk Energi & Kylanalys AB and Svenska Kyltekniska Föreningen. Adrián Mota-Babiloni would like to acknowledge the funding received from the Plan for the promotion of research of the University Jaume I for the year 2016 [Grant number POSDOC/2016/23].

References

[1] United Nations Environment Programme (UNEP). Twenty-Eighth Meeting of the Parties to the Montreal Protocol on Substances that Deplete the Ozone Layer. Decision XXVIII/--- Further Amendment of the Montreal Protocol. 2016:1–9.

[2] The European Parliament and the Council of the European Union. Regulation (EU) No 517/2014 of the European Parliament and the Council of 16 April 2014 on fluorinated greenhouse gases and repealing Regulation (EC) No 842/2006. Off J Eur Union 2014;150:195–230.

[3] Mota-Babiloni A, Makhnatch P, Khodabandeh R. Recent investigations in HFCs substitution with lower GWP synthetic alternatives: Focus on energetic performance and environmental impact. Int J Refrig 2017;82. doi:10.1016/j.ijrefrig.2017.06.026.

[4] Yang Z, Wu X. Retrofits and options for the alternatives to HCFC-22. Energy 2013;59:1–21. doi:10.1016/J.ENERGY.2013.05.065.

[5] Li G, Eisele M, Lee H, Hwang Y, Radermacher R. Experimental investigation of energy and exergy performance of secondary loop automotive air-conditioning systems using low-GWP (global warming potential) refrigerants. Energy 2014;68:819–31. doi:10.1016/J.ENERGY.2014.01.018.

[6] Zilio C, Brown JS, Schiochet G, Cavallini A. The refrigerant R1234yf in air conditioning systems. Energy 2011;36:6110–20. doi:10.1016/J.ENERGY.2011.08.002.

[7] Mota-Babiloni A, Navarro-Esbrí J, Barragán Á, Molés F, Peris B. Drop-in energy performance evaluation of R1234yf and R1234ze(E) in a vapor compression system as R134a replacements. Appl Therm Eng 2014;71. doi:10.1016/j.applthermaleng.2014.06.056.

[8] IPCC. The Physical Science Basis. Contribution of Working Group I to the Fifth Assessment Report of the Intergovernmental Panel on Climate Change. Clim. Chang. 2013, 2013, p. 1535. doi:10.1017/CBO9781107415324.

[9] Feng B, Yang Z, Zhai R. Experimental study on the influence of the flame retardants on the flammability of R1234yf. Energy 2018;143:212–8. doi:10.1016/J.ENERGY.2017.10.078.

[10] Yang Z, Wu X, Tian T. Flammability of Trans-1, 3, 3, 3-tetrafluoroprop-1-ene and its binary blends. Energy 2015;91:386–92. doi:10.1016/J.ENERGY.2015.08.037.

[11] Davis SG, Pagliaro JL, Debold TF, van Wingerden M, van Wingerden K. Flammability and explosion characteristics of mildly flammable refrigerants. J Loss Prev Process Ind 2017;49:662–74. doi:10.1016/J.JLP.2017.05.019.

[12] Mota-Babiloni A, Navarro-Esbrí J, Mendoza-Miranda JM, Peris B. Experimental evaluation of system modifications to increase R1234ze(E) cooling capacity. Appl Therm Eng 2017;111. doi:10.1016/j.applthermaleng.2016.09.175.

[13] Mota-Babiloni A, Navarro-Esbrí J, Barragán-Cervera A, Molés F, Peris B. Drop-in analysis of an internal heat exchanger in a vapour compression system using R1234ze(E) and R450A as alternatives for R134a. Energy 2015;90. doi:10.1016/j.energy.2015.06.133.

[14] Mota-Babiloni A, Makhnatch P, Khodabandeh R, Navarro-Esbrí J. Experimental assessment of R134a and its lower GWP alternative R513A. Int J Refrig 2017;74. doi:10.1016/j.ijrefrig.2016.11.021.

[15] Mendoza-Miranda JM, Mota-Babiloni A, Ramírez-Minguela JJ, Muñoz-Carpio VD, Carrera-Rodríguez M, Navarro-Esbrí J, et al. Comparative evaluation of R1234yf, R1234ze(E) and R450A as alternatives to R134a in a variable speed reciprocating compressor. Energy 2016;114. doi:10.1016/j.energy.2016.08.050.

[16] Llopis R, Sánchez D, Cabello R, Catalán-Gil J, Nebot-Andrés L. Experimental analysis of R-450A and R-513A as replacements of R-134a and R-507A in a medium temperature commercial refrigeration system. Int J Refrig 2017;84:52–66. doi:10.1016/J.IJREFRIG.2017.08.022.

[17] Makhnatch P, Mota-Babiloni A, Khodabandeh R. Experimental study of R450A drop-in performance in an R134a small capacity refrigeration unit. Int J Refrig 2017;84. doi:10.1016/j.ijrefrig.2017.08.010.

[18] Ahamed JU, Saidur R, Masjuki HH. A review on exergy analysis of vapor compression refrigeration system. Renew Sustain Energy Rev 2011;15:1593–600. doi:10.1016/J.RSER.2010.11.039.

[19] Du Z, Jin X, Fan B. Evaluation of operation and control in HVAC (heating, ventilation and air conditioning) system using exergy analysis method. Energy 2015;89:372–81. doi:10.1016/J.ENERGY.2015.05.119.

[20] Özgür AE, Kabul A, Kizilkan Ö. Exergy analysis of refrigeration systems using an alternative refrigerant (HFO-1234yF) to R-134a. Int J Low-Carbon Technol 2014;9:56–62. doi:10.1093/ijlct/cts054.

[21] Golzari S, Kasaeian A, Daviran S, Mahian O, Wongwises S, Sahin AZ. Second law analysis of an automotive air conditioning system using HFO-1234yf, an environmentally friendly refrigerant . Int J Refrig 2017;73:134–43. doi:10.1016/j.ijrefrig.2016.09.009.

[22] Yataganbaba A, Kilicarslan A, Kurtbaş I. Exergy analysis of R1234yf and R1234ze as R134a replacements in a two evaporator vapour compression refrigeration system. Int J Refrig 2015;60:26–37. doi:10.1016/j.ijrefrig.2015.08.010.

[23] Cho H, Park C. Experimental investigation of performance and exergy analysis of automotive air conditioning systems using refrigerant R1234yf at various compressor speeds. Appl Therm Eng 2016;101:30–7. doi:10.1016/j.applthermaleng.2016.01.153.

[24] Belman-Flores JM, Rangel-Hernández VH, Usón S, Rubio-Maya C. Energy and exergy analysis of R1234yf as drop-in replacement for R134a in a domestic refrigeration system. Energy 2017;132:116–25. doi:10.1016/j.energy.2017.05.074.

[25] Kabeel AE, Khalil A, Bassuoni MM, Raslan MS. Comparative experimental study of low GWP alternative for R134a in a walk-in cold room. Int J Refrig 2016;69:303–12. doi:10.1016/j.ijrefrig.2016.06.017.

[26] Ben Jemaa R, Mansouri R, Boukholda I, Bellagi A. Energy and exergy investigation of R1234ze as R134a replacement in vapor compression chillers. Int J Hydrogen Energy 2017;42:12877–87. doi:10.1016/j.ijhydene.2016.12.010.

[27] Pérez-García V, Belman-Flores JM, Rodríguez-Muñoz JL, Rangel-Hernández VH, Gallegos-Muñoz A. Second law analysis of a mobile air conditioning system with internal heat exchanger using low GWP refrigerants. Entropy 2017;19. doi:10.3390/e19040175.

[28] Lemmon EW, Huber ML, McLinden MO. NIST Standard Reference Database 23. Ref Fluid Thermodyn Transp Prop (REFPROP), Version 91 2013.

[29] Moran MJ, Shapiro HN, Boettner DD, Bailey M. Fundamentals of Engineering Thermodynamics. 2010.

[30] Taylor BN, Kuyatt CE. NIST Technical Note 1297 1994 Edition, Guidelines for Evaluating and Expressing the Uncertainty of NIST Measurement Results. Natl Inst Stand Technol 1994:1–20.

Appendix A

In this appendix section, the condensing and evaporating experimental temperatures for R134a and R513A is reported. Likewise, the uncertainty of exergy efficiency and

653 exergy destruction rate for the global system and its main four components is also
654 provided.
655
656 Table A1. Uncertainty of the estimated parameters for R134a and R513A.
657
658

Table 1. Main characteristics of 513A and R134a.

	R513A	R134a
Molecular weight [g mol^{-1}]	108.4	102
ASHRAE safety class	A1	A1
ODP	0	0
GWP	573	1300
Critical temperature [°C]	96.50	101.10
Critical pressure [MPa]	3.76	4.05
Normal boiling point [°C]	-29.60	-26.10
Glide at 0.1 MPa [K]	0.1	0.0
Liquid density at 0°C [kg m^{-3}]	1221.9	1294.8
Vapor density at 25°C [kg m^{-3}]	37.63	32.35

Table 2. Measurements collected in the experimental refrigeration setup.

Measurement	**Sensor**	**Uncertainty**	**Range**
Temperature	T type thermocouple	±0.11 K	[-60 – 100] °C
Discharge pressure	Pressure sensor	±0.08% (full scale	[0 – 2.1] MPa
Suction pressure	transducer	best straight line)	[0 – 1.1] MPa
Evaporator pressure drop	Differential Pressure sensor	±0.25% (reading)	
Refrigerant mass flow rate	Coriolis type flowmeter	±0.5% (reading)	[0-20] g s^{-1}
Electric power use of the motor-compressor set	Configurable multi transducer	±0.2% (reading)	[0 – 750] W
Electric power use of the heaters			[0 – 3000] W

Table 3. Exergy destruction and efficiency equations for each component analyzed.

Component	Exergy destruction	Exergy efficiency
Compressor	$\dot{E}_{d,comp} = \left(1 - \frac{T_0}{T_{wall}}\right)\dot{Q}_c - \dot{W}_{comp} + \dot{E}_{suc} - \dot{E}_{disc}$ $\dot{E}_{suc} = \dot{m}_{ref}[(h_{suc} - h_0) - T_0(s_{suc} - s_0)]$ $\dot{E}_{disc} = \dot{m}_{ref}[(h_{disc} - h_0) - T_0(s_{disc} - s_0)]$	$\eta_{ex,comp} = 1 - \frac{\dot{E}_{d,comp}}{\dot{W}_{comp}}$
Condenser	$\dot{E}_{d,cond} = (\dot{E}_{in} - \dot{E}_{out})_{cond} + (\dot{E}_{in} - \dot{E}_{out})_{water}$ $\dot{E}_{in,cond} = \dot{m}_{ref}[(h_{in} - h_0) - T_0(s_{in} - s_0)]$ $\dot{E}_{out,cond} = \dot{m}_{ref}[(h_{out} - h_0) - T_0(s_{out} - s_0)]$ $\dot{E}_{in,water} = \dot{m}_{water}[(h_{in} - h_0) - T_0(s_{out} - s_0)]$ $\dot{E}_{out,water} = \dot{m}_{water}[(h_{out} - h_0) - T_0(s_{out} - s_0)]$	$\eta_{ex,cond} = 1 - \frac{\dot{E}_{d,cond}}{(\dot{E}_{in} - \dot{E}_{out})_{cond}}$
TXV	$\dot{E}_{d,TXV} = \dot{E}_{in,TXV} - \dot{E}_{out,TXV}$ $\dot{E}_{in,TXV} = \dot{m}_{ref}[(h_{in} - h_0) - T_0(s_{in} - s_0)]$ $\dot{E}_{out,TXV} = \dot{m}_{ref}[(h_{out} - h_0) - T_0(s_{out} - s_0)]$	$\eta_{ex,TXV} = 1 - \frac{\dot{E}_{d,TXV}}{\dot{E}_{in,TXV}}$
Evaporator	$\dot{E}_{d,evap} = (\dot{E}_{in} - \dot{E}_{out})_{evap} + (\dot{E}_{in} - \dot{E}_{out})_{brine}$ $\dot{E}_{in,evap} = \dot{m}_{ref}[(h_{in} - h_0) - T_0(s_{in} - s_0)]$ $\dot{E}_{out,evap} = \dot{m}_{ref}[(h_{out} - h_0) - T_0(s_{out} - s_0)]$ $\dot{E}_{in,brine} = \dot{m}_{brine}[(h_{in} - h_0) - T_0(s_{out} - s_0)]$ $\dot{E}_{out,brine} = \dot{m}_{brine}[(h_{out} - h_0) - T_0(s_{out} - s_0)]$	$\eta_{ex,evap} = 1 - \frac{\dot{E}_{d,evap}}{(\dot{E}_{in} - \dot{E}_{out})_{evap}}$

Table 4. Global and components exergy efficiency at 30°C condensing temperature.

Refrigerant	Measure	Compressor	Condenser	TXV	Evaporator	Global
R134a	Max	0.460	0.986	0.972	0.670	0.264
	Ave	0.437	0.962	0.946	0.574	0.240
	Min	0.400	0.922	0.913	0.425	0.189
R513A	Max	0.470	0.959	0.987	0.666	0.263
	Ave	0.452	0.946	0.969	0.583	0.248
	Min	0.415	0.939	0.915	0.427	0.217

Table 5. Global and components exergy efficiency at 35°C condensing temperature.

Refrigerant	Measure	Compressor	Condenser	TXV	Evaporator	Global
R134a	Max	0.497	0.825	0.959	0.684	0.238
	Ave	0.449	0.808	0.931	0.584	0.223
	Min	0.383	0.774	0.900	0.419	0.199
R513A	Max	0.507	0.790	0.965	0.678	0.243
	Ave	0.479	0.733	0.931	0.608	0.223
	Min	0.429	0.623	0.899	0.463	0.176

Table A1. Uncertainty of the estimated parameters for R134a and R513A.

			Uncertainty (±)									
			Global		Compressor		Condenser		TXV		Evaporator	
Refrigerant	T_{cond} [°C]	T_{evap} [°C]	η_{ex} [-]	$\dot{E}_d$ [W]	η_{ex} [-]	$\dot{E}_d$ [W]	η_{ex} [-]	$\dot{E}_d$ [W]	η_{ex} [-]	$\dot{E}_d$ [W]	η_{ex} [-]	$\dot{E}_d$ [W]
R134a	30.0	-15.0	0.0011	1.1	0.0058	2.7	0.0164	0.4	0.0005	0.3	0.0112	2.0
R134a	30.1	-12.4	0.0012	1.2	0.0053	2.6	0.0177	0.4	0.0005	0.3	0.0100	1.9
R134a	30.0	-9.8	0.0013	1.2	0.0050	2.4	0.0194	0.4	0.0004	0.2	0.0086	1.8
R134a	30.0	-7.7	0.0013	1.2	0.0047	2.3	0.0199	0.5	0.0004	0.2	0.0079	1.7
R134a	29.9	-5.3	0.0018	1.3	0.0044	2.2	0.0242	0.5	0.0004	0.2	0.0069	1.6
R134a	30.0	-2.3	0.0019	1.4	0.0039	2.0	0.0240	0.5	0.0003	0.2	0.0059	1.5
R134a	30.1	0.1	0.0021	1.4	0.0037	1.9	0.0250	0.6	0.0003	0.2	0.0052	1.4
R134a	30.0	2.7	0.0022	1.4	0.0034	1.8	0.0266	0.6	0.0003	0.2	0.0048	1.3
R134a	30.0	5.2	0.0023	1.5	0.0031	1.7	0.0283	0.7	0.0002	0.2	0.0046	1.2
R134a	35.1	-14.82	0.0009	1.12	0.0060	2.91	0.0075	0.64	0.0006	0.34	0.0127	1.98
R134a	35.1	-12.01	0.0010	1.13	0.0055	2.74	0.0077	0.63	0.0005	0.30	0.0110	1.85
R134a	35.0	-9.90	0.0010	1.14	0.0051	2.60	0.0080	0.62	0.0005	0.27	0.0102	1.76
R134a	35.0	-7.54	0.0011	1.17	0.0049	2.47	0.0083	0.61	0.0005	0.28	0.0085	1.63
R134a	35.0	-4.78	0.0010	1.15	0.0045	2.32	0.0041	0.52	0.0004	0.27	0.0068	1.51
R134a	34.9	-2.51	0.0013	1.22	0.0042	2.19	0.0090	0.64	0.0004	0.24	0.0061	1.43
R134a	35.0	-0.04	0.0015	1.25	0.0039	2.07	0.0092	0.67	0.0004	0.23	0.0054	1.33
R134a	35.0	2.75	0.0016	1.28	0.0036	1.93	0.0093	0.71	0.0003	0.21	0.0049	1.23
R134a	35.1	5.11	0.0017	1.31	0.0033	1.83	0.0095	0.74	0.0003	0.20	0.0046	1.15
R513A	30.0	-15.0	0.0012	1.34	0.0064	3.06	0.0146	0.46	0.0005	0.31	0.0096	2.18
R513A	30.1	-12.5	0.0013	1.35	0.0059	2.87	0.0138	0.49	0.0005	0.30	0.0085	2.01
R513A	30.0	-10.0	0.0014	1.37	0.0055	2.72	0.0146	0.51	0.0004	0.26	0.0078	1.91
R513A	30.0	-7.6	0.0014	1.38	0.0051	2.58	0.0136	0.54	0.0004	0.26	0.0069	1.77
R513A	29.9	-5.3	0.0015	1.40	0.0048	2.43	0.0150	0.56	0.0004	0.23	0.0062	1.67
R513A	30.0	-2.7	0.0016	1.42	0.0043	2.27	0.0145	0.62	0.0003	0.21	0.0055	1.53
R513A	30.1	0.0	0.0017	1.45	0.0041	2.15	0.0154	0.65	0.0003	0.19	0.0051	1.42
R513A	30.0	2.6	0.0018	1.48	0.0037	2.02	0.0154	0.70	0.0003	0.18	0.0047	1.32
R513A	30.0	5.1	0.0020	1.52	0.0035	1.91	0.0177	0.75	0.0002	0.15	0.0045	1.23
R513A	35.1	-14.89	0.0010	1.32	0.0065	0.72	0.0066	0.72	0.0005	0.36	0.0099	2.12
R513A	35.1	-12.39	0.0011	1.34	0.0061	0.73	0.0067	0.73	0.0005	0.35	0.0088	1.97
R513A	35.0	-10.18	0.0012	1.35	0.0057	0.72	0.0068	0.72	0.0005	0.33	0.0080	1.85
R513A	35.0	-7.59	0.0013	1.37	0.0053	0.71	0.0071	0.71	0.0004	0.29	0.0071	1.74
R513A	35.0	-4.95	0.0013	1.38	0.0050	0.73	0.0072	0.73	0.0004	0.28	0.0063	1.60
R513A	34.9	-2.47	0.0014	1.39	0.0045	0.75	0.0071	0.75	0.0004	0.25	0.0059	1.48
R513A	35.0	-0.15	0.0015	1.42	0.0043	0.76	0.0074	0.76	0.0003	0.22	0.0054	1.39
R513A	35.0	2.39	0.0016	1.46	0.0040	0.80	0.0075	0.80	0.0003	0.21	0.0048	1.29
R513A	35.1	4.93	0.0017	1.49	0.0037	0.84	0.0074	0.84	0.0003	0.20	0.0046	1.19

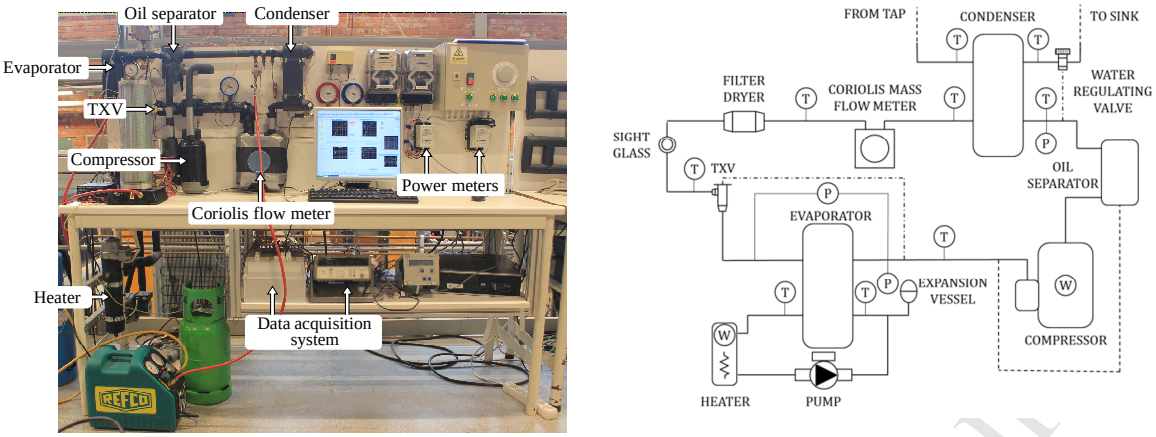

a) b)

Figure 1. a) Experimental setup and b) schematic diagram of its main components.

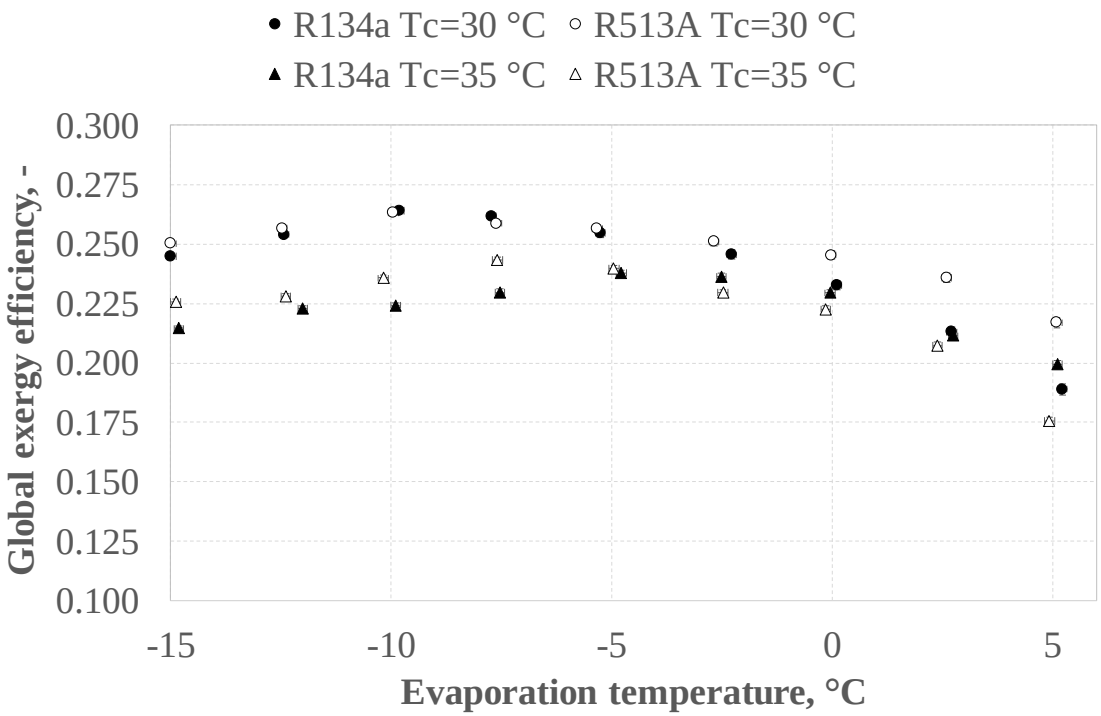

a) Exergy efficiency

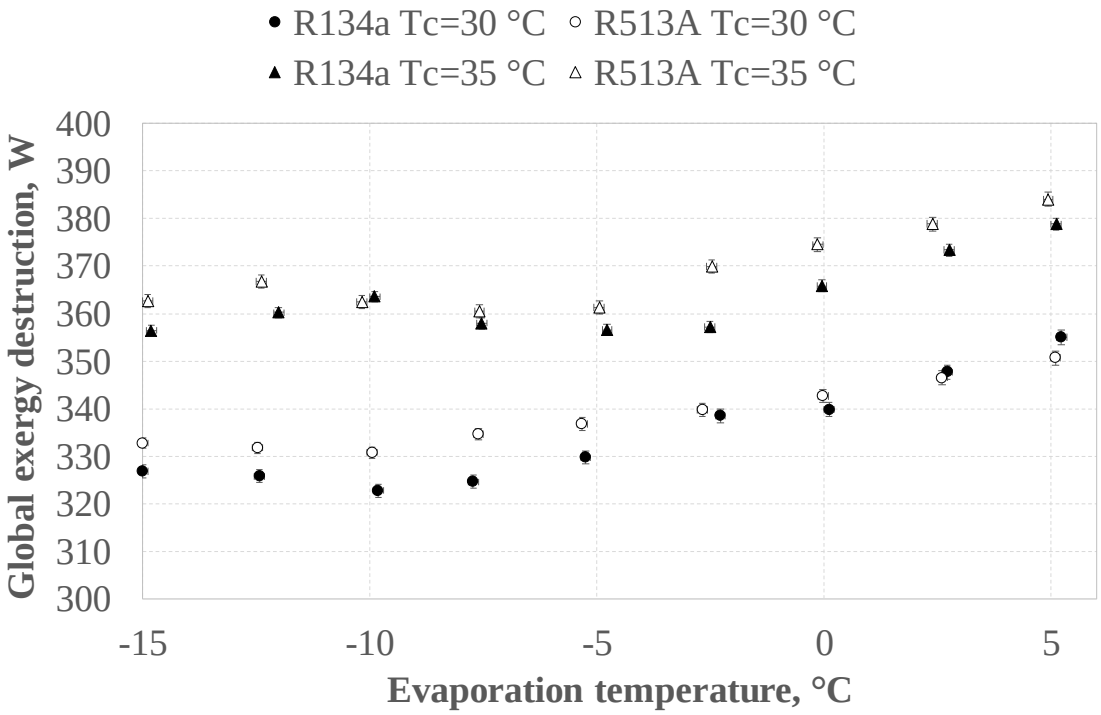

b) Exergy destruction

Figure 2. Global exergy performance vs evaporation temperature.

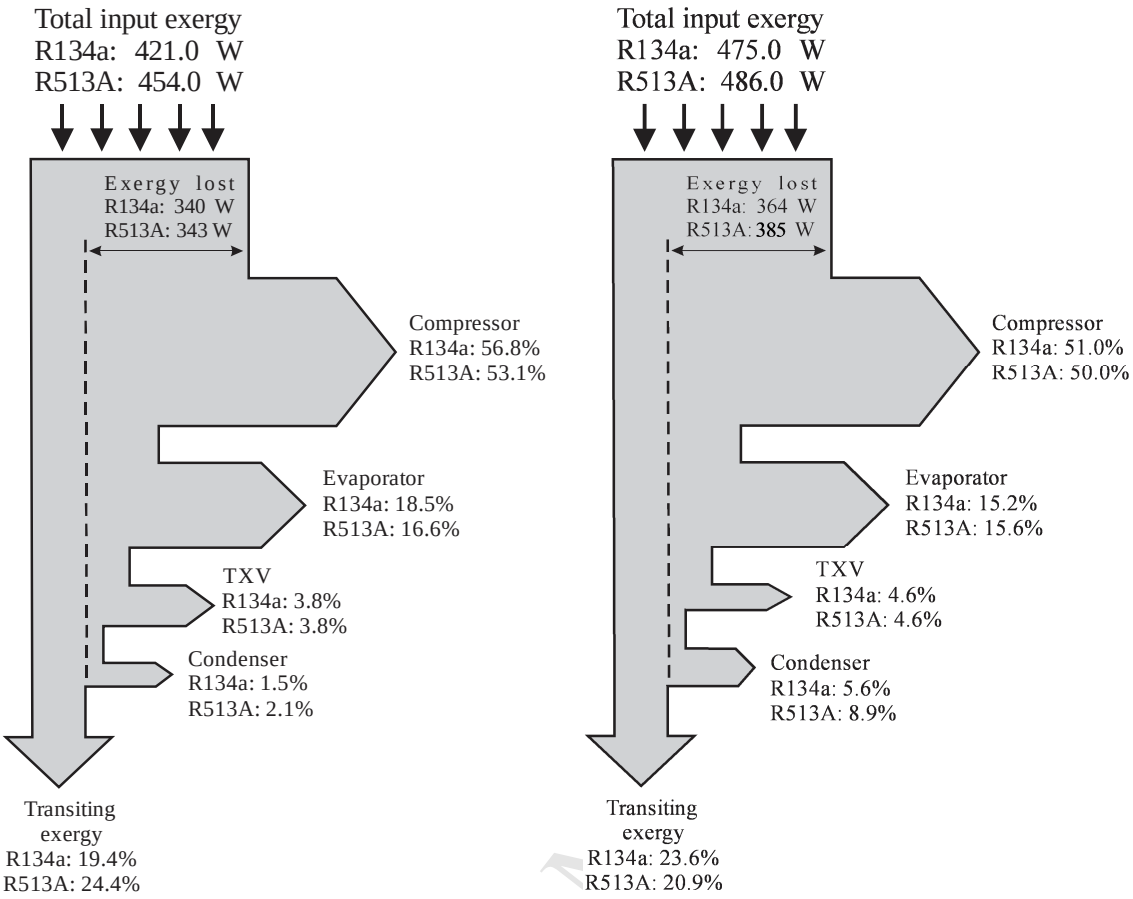

Figure 3. Exergy flow diagram for the refrigeration system, at a) T_{cond}=30°C, b) T_{cond}=35°C.

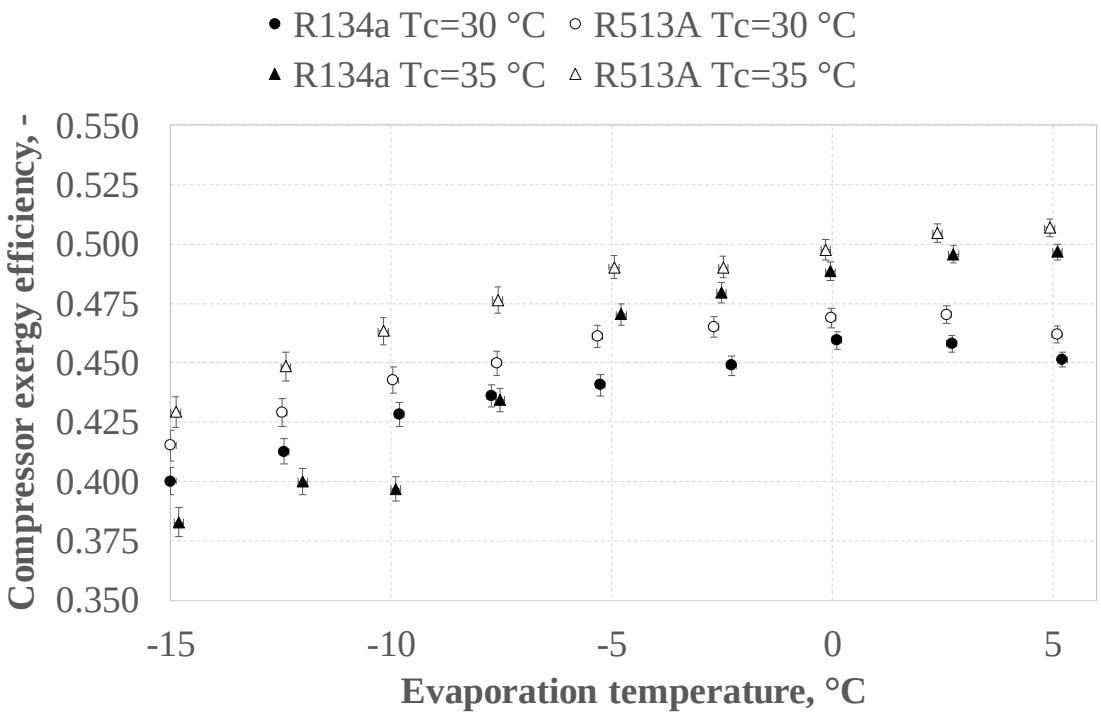

a)

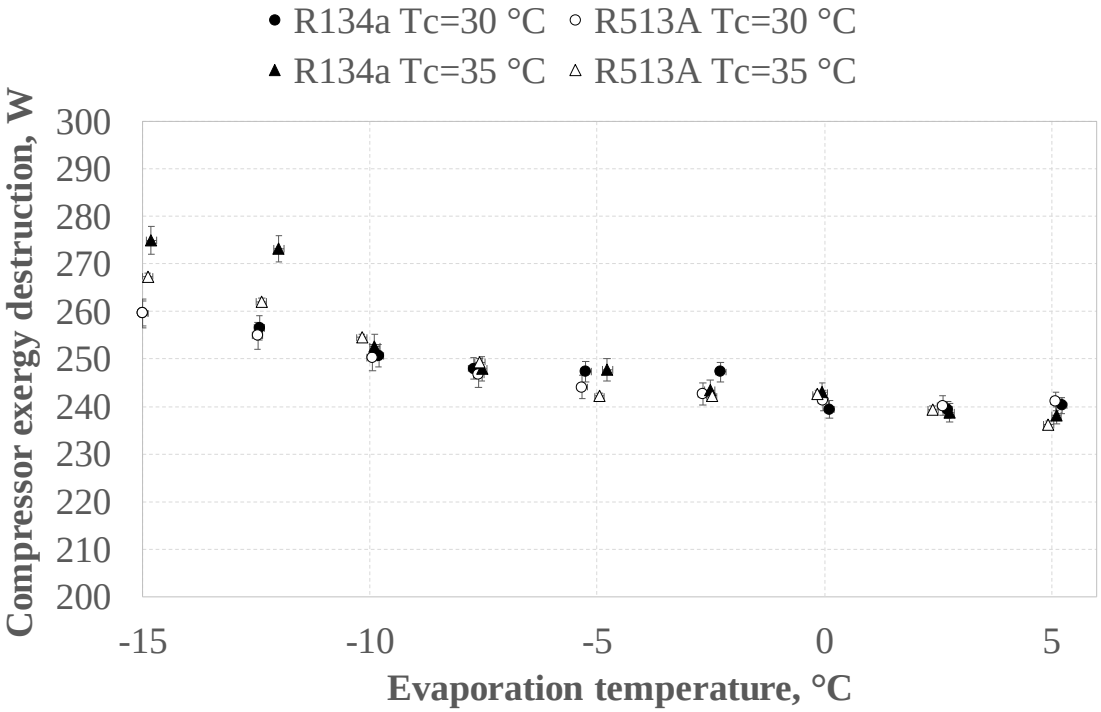

b)

Figure 4. Exergy performance of the compressor, a) efficiency and b) destruction

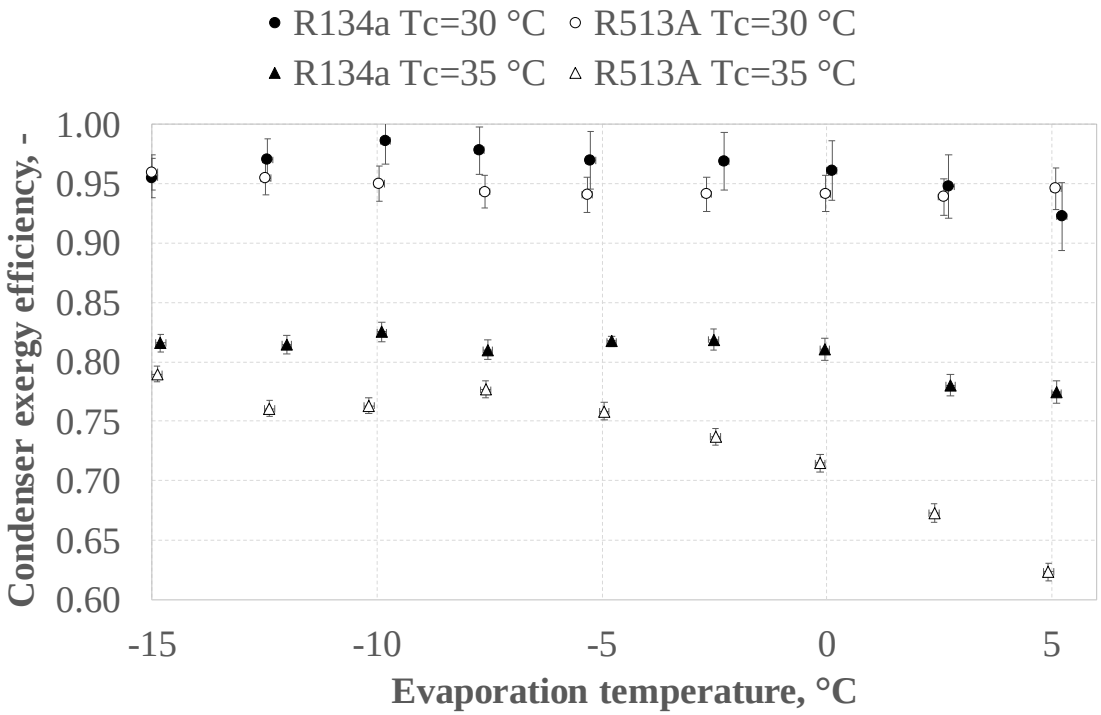

a)

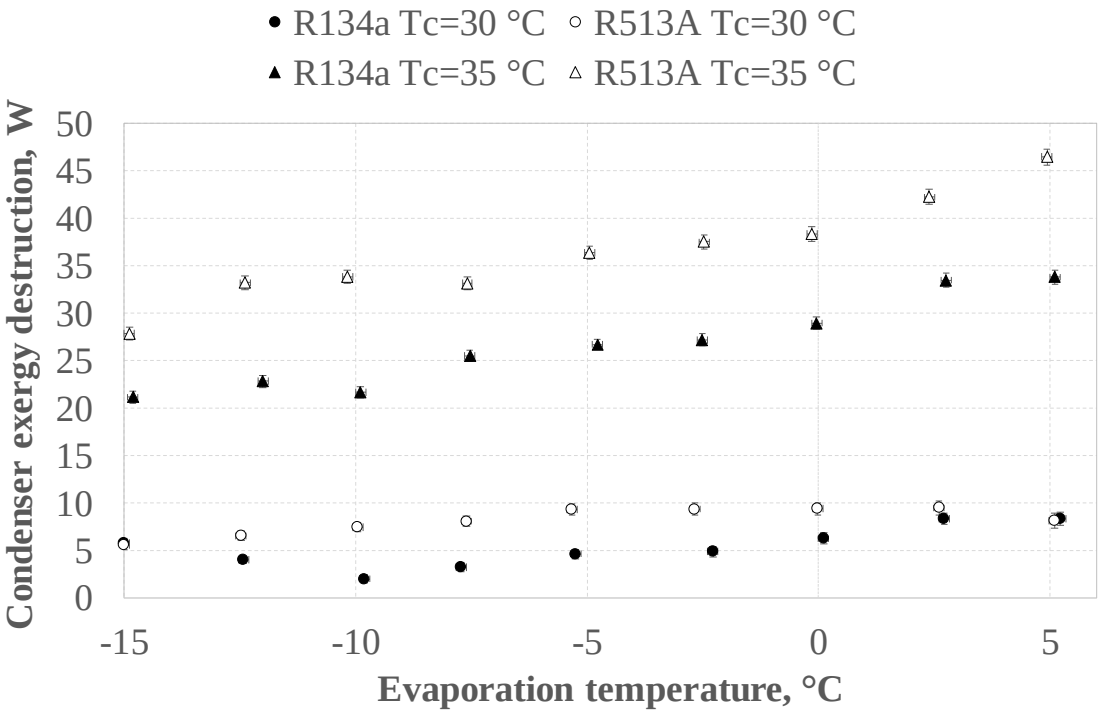

b)

Figure 5. Exergy performance of the condenser, a) efficiency and b) destruction.

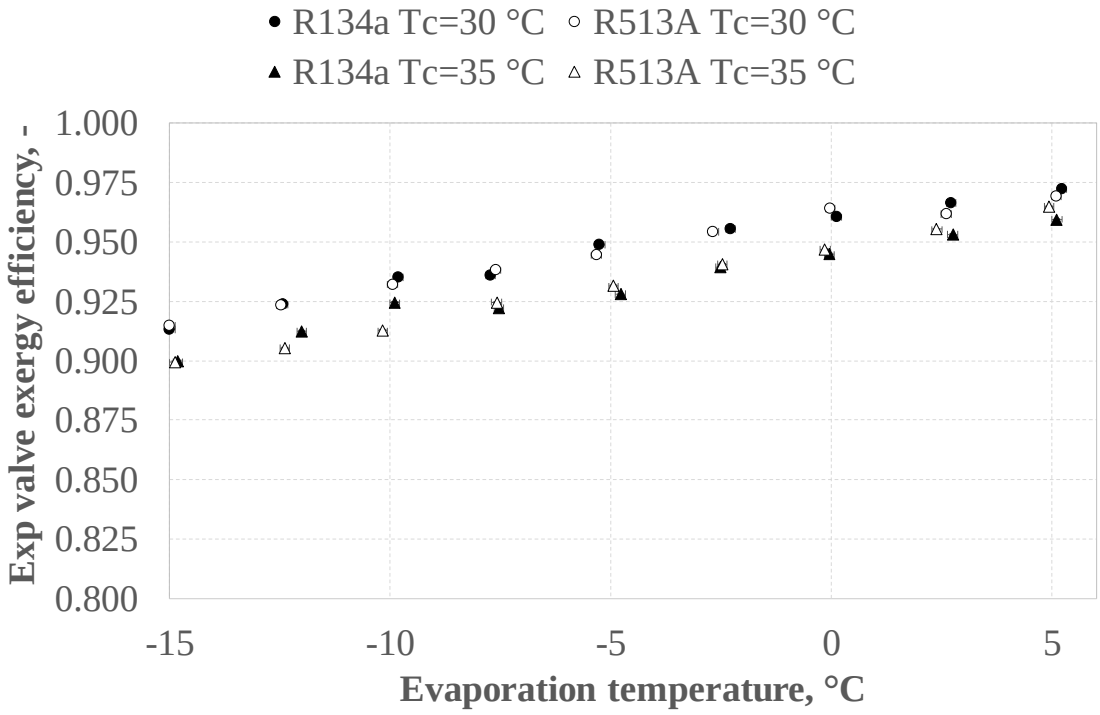

a)

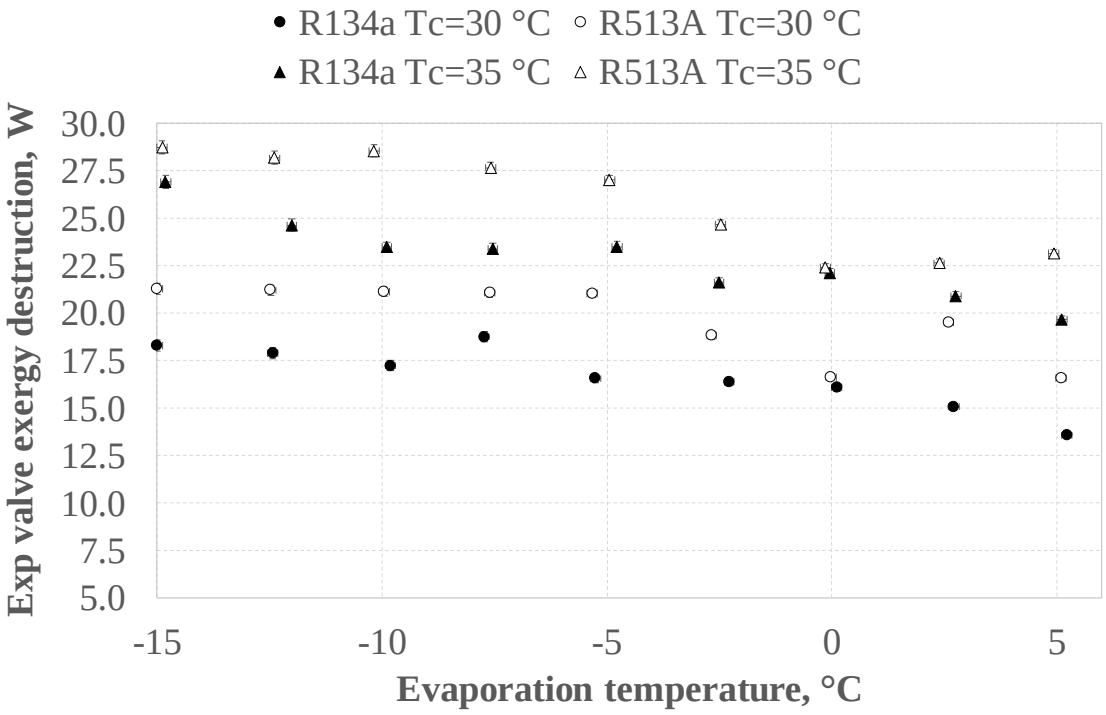

b)

Figure 6. Exergy performance of the expansion valve, a) efficiency and b) destruction.

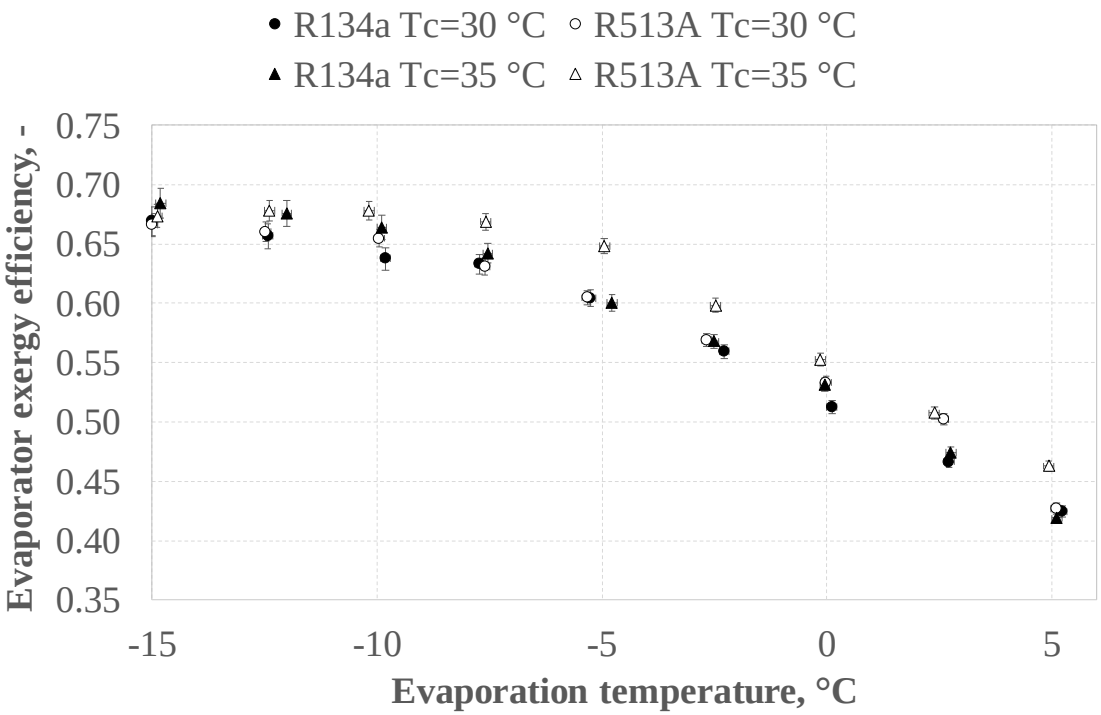

a)

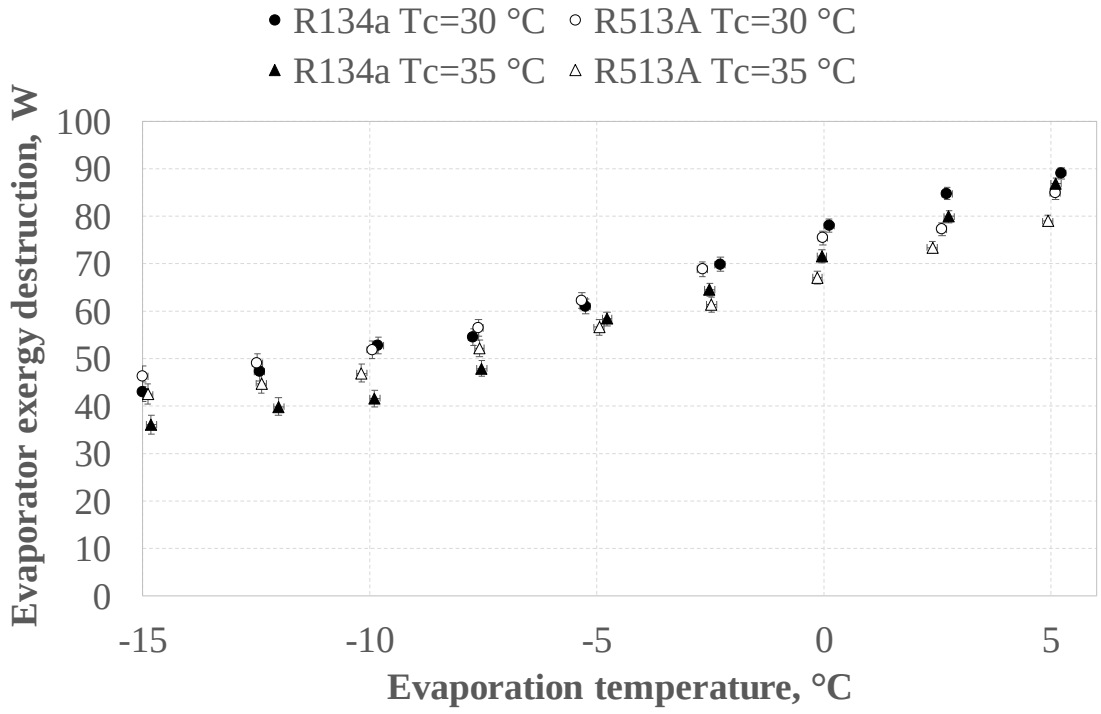

b)

Figure 7. Exergy performance of the evaporator, a) efficiency and b) destruction.

- The experimental results on the exergy behavior of R513A versus R134a are discussed.

- The global exergy efficiency of R513A is slightly higher than that of R134a.

- The component that cause higher irreversibility and hence lower exergy efficiency is the compressor.

- The second-law analysis confirmed that R513A does not needs redesign to be used in R134a refrigeration systems.